phys. stat. sol. (a) **175**, 317 (1999)

Subject classification: 73.30.+y; 61.16.Ch; 78.90.+t; S7.12; S7.15

Interface Applications of Scanning Near-Field Optical Microscopy with a Free Electron Laser

A. CRICENTI (a), R. GENEROSI (a), P. PERFETTI (a), G. MARGARITONDO (b), J. ALMEIDA (b+), J. M. GILLIGAN (c), N. H. TOLK (c), C. COLUZZA (d), M. SPAJER (e), D. COURJON (e), and I. D. AGGARWAL (f)

(a) Istituto di Stuttura della Materia, CNR, via Fosso del Cavaliere 100, I-00133 Roma, Italy

(b) Institut de Physique Appliquée, Ecole Polytecnique Fédérale, CH-1015 Lausanne, Switzerland

(c) Department of Physics and Astronomy, Vanderbilt University, Nashville, Tennessee 37235, USA

(d) Dipartimento di Fisica, Universita di Roma "La Sapienza", P. le A. Moro 2, I-00185 Roma, Italy

(e) Laboratoire d'Optique, P. M. Duffieux, Université de Franche-Comté, F-25030 Besançon, France

(f) Optical Science Division, U.S. Naval Research Laboratory, 4555 Overlook Avenue SE, Washington, D.C. 20375, USA

(Received May 8, 1999)

The study of semiconductor interfaces and of solid interfaces in general requires novel instrument capable to investigate the lateral fluctuations of properties on a microscopic scale. We present the first result of a major effort in that framework, whose main objective is the exploitation of the unique characteristics of free electron laser (FEL) infrared sources. The background was provided by our previous development of FEL-based techniques to measure interface barriers with high accuracy and reliability. Quite recently, we were able to implement similar investigations with high lateral resolution. The key elements were the use of a small-tip optics fiber and its coupling with a scanning module; in this way, we achieved and verified the condition of near-field microscopy – including a lateral resolution much below the wavelength value. Our discussion includes a presentation of the first scanning near-field optical microscopy (SNOM) images obtained with an FEL and data on small and microscopic-scale fluctuations of semiconductor interface barriers. The likely development of this exciting new field will also be discussed, in particular considering the new proposals for powerful FELs in the low-wavelength spectral range.

1. Introduction

The recent interest in semiconductor interface research has been gradually shifting to the problem of lateral fluctuations [1 to 3]. Laterally-resolved photoemission experiments clearly demonstrated that crucially important interface parameters – such as Schottky barriers and heterojunction band discontinuities – can fluctuate in the interface plane [1]. On the other hand, the behavior of semiconductor devices is probably dominated by the points with the weakest barriers. Hence, the necessity to move from "averaged" studies of the interfaces to spatially-resolved investigations.

The substantial progress in studying this issue notwithstanding, there still exists in this domain a severe limitation. The laterally-resolved photoemission probes that can investigate this problem have limited energy resolution and consequently limited accuracy and sensitivity in measuring the barrier fluctuations [1]. The problem is solved by Ballistic Electron Emission Microscopy (BEEM) technique [4] only in part, and novel approaches are highly desirable.

Quite recently, a new opportunity emerged to solve this critical problem: the combination of two established techniques results in a novel approach to obtain barrier fluctuation measurements with high lateral resolution and high energy resolution. The two ingredients are the Free Electron Laser Internal Photoemission (FELIPE) Technique [5] and Scanning Near-Field Optical Microscopy (SNOM) [6 to 8]. We briefly review the status of this effort, including the first measurements of barrier fluctuations and the first SNOM images ever obtained with a free electron laser (FEL) [8]. Our discussion ends with an assessment of the likely future developments of this promising domain, in particularly considering the forthcoming implementation of new FEL sources.

2. The FELIPE (Free Electron Laser Internal Photoemission) Technique

Interface barrier measurements with optics-based techniques typically require infrared photons. The best available infrared sources are the FELs. Sources of this kind have been operated for many years, but their practical applications are still somewhat scarce. The first positive tests [5] show that this is not due to some insurmountable difficulty.

The few existing examples of FEL-based experiments are in fact very interesting and encouraging. This is true, in particular, for experiments on semiconductor interfaces. The first program in this field was implemented at the Vanderbilt Free Electron Laser Center [5], and resulted in the development of the internal-photoemission technique known as "FELIPE".

The basic philosophy of this technique [5] is quite simple (see Fig. 1): the semiconductor interface barrier to be measured is inserted in a photocurrent detecting circuit. Infrared radiation can excite carriers over the barrier thereby producing a photocurrent. The barrier height is then simply given by the photocurrent threshold. The approach can be applied both to Schottky barriers and to heterojunction band discontinuities [5].

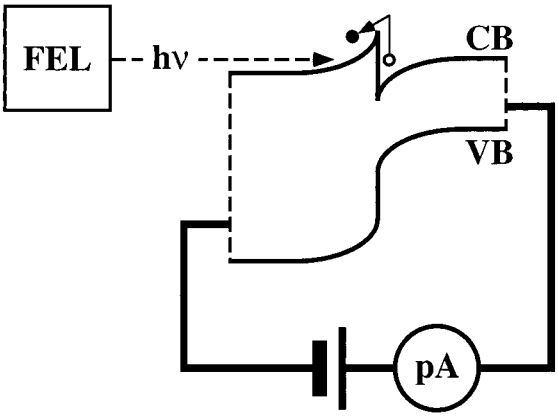

Fig. 1. Schematic explanation of the FELIPE technique: given an appropriate doping and a suitable, intense tunable photon source, a photocurrent can be excited across a semiconductor–semiconductor interface [5]. In this case, the conduction band discontinuity corresponds to a photocurrent threshold and can be measured from it. Similar schemes apply to other interfaces, e.g., metal–semiconductor interfaces

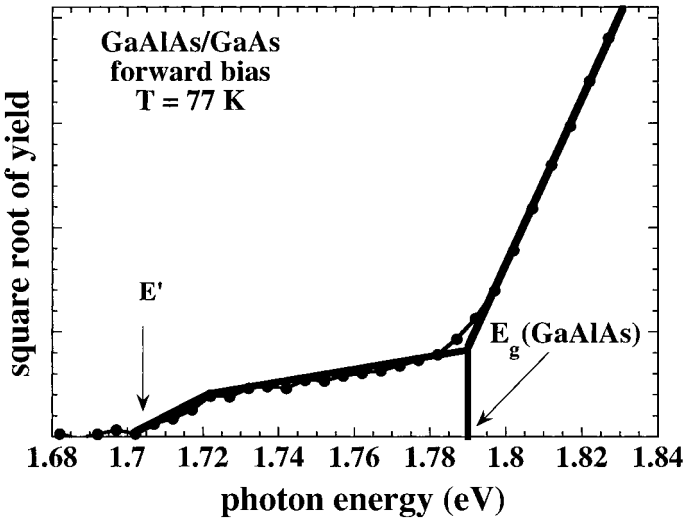

Fig. 2. Example of an early FELIPE spectrum (Ref. ([5]) taken with the Vanderbilt FEL, with features corresponding to the GaAlAs energy gap and to one of the photocurrent barriers of a GaAlAs/GaAs interface

The role of an FEL source in this approach is to enhance its effectiveness and flexibility by providing tunable and intense radiation over a broad spectral range. In order to appreciate the importance of this role, one must consider the practical problems in the implementation of the FELIPE approach [5]. In addition to barrier-related threshold, one normally detects several other photocurrent spectral features, and it is essential to distinguish these spurious contributions from those actually related to barriers.

This is possible by performing experiments over a rather broad spectral range, thus obtaining an overall picture of the different types of spectral contributions to analyze and identify them. A narrow-band approach, on the other hand, can be potentially misleading: one could detect a spurious threshold and attribute it to the barrier of interest, whereas the real barrier-related threshold could be just out of reach.

The superior performances of the Vanderbilt University FEL stimulated a few years ago the development of the first experimental program in this area. The program has been in operation for several years, producing routine experimental measurements of semiconductor interface barriers with a few meV accuracy. Fig. 2 shows [5] an example of results from the FELIPE approach.

3. First Laterally-Resolved Tests

Although FELIPE experiments solved the problem of measuring interface barriers with high accuracy and reliability, they did not eliminate the other basic limitation of interface research: the lack of lateral resolution. This naturally led [7] to the proposal of using a combination of internal photoemission (IPE) and near-field optics. The first successful test on Pt–GaP [7] did not reach near-field conditions, but did provide evidence of lateral Schottky barrier height fluctuations on a smaller energy scale than any other previous experiment.

Specifically, this approach enabled us to measure IPE Pt/n–GaP(001) interface photocurrents with high lateral resolution. We observed photocurrent intensity lateral variations which did not match topographic features of shear-force microimages, and revealed fluctuations in the electron–hole recombination rate. We also detected lateral variations of the Pt–GaP Schottky barrier, of 3 to 8 meV on the lateral scale of less than 1 μm.

We achieved high lateral resolution in the internal photoemission measurements by illuminating the sample with a small light spot, based on the SNOM technique [6 to 8]. The light source for these initial tests was not an FEL but a tunable dc Ti–sapphire laser or a solid state laser diode (fixed photon energy at 1.512 eV). The Ti–sapphire laser provided tunable light in the interval 1.319 to 1.53 eV. The overall photon energy resolution was ≈1 meV, as derived from full width at half maximum of luminescence lines in test samples.

The maximum power output of the dc Ti–sapphire laser was 100 to 300 mW. The effective power in the fiber was about 30 mW. The light beam was chopper-modulated and split in two; one part was detected with a Si avalanche photodiode, the other focused over the metal-covered side of the sample (see below).

The tip of the optical fiber was stretched and aluminum-coated to concentrate the light beam into a 50 nm wide pinhole. Piezoelectric translators implemented the vertical approach up to the near-field condition, and the X–Y scanning over a rectangular area of size ranging from 8 to 30 μm. The experiments were performed with a constant 10 nm tip-to-sample distance; this resulted in a topographic vertical resolution of about 1 nm. The tip–sample distance was controlled by a shear-force feedback system, described in Ref. [9]. The Ti–sapphire laser high power induced a partial damage of the metallic coating of the fiber tip, as observed by scanning electron microscopy.

Photocurrent microimages were obtained by detecting the photocurrent signal while scanning the beam over the sample. The photocurrent was revealed with a standard lock-in technique. Topographic images were obtained by measuring the shear-force signal with a synchronous detection including a piezoelectric oscillator and a lock-in amplifier [9, 10].

From the smallest visible features, we estimated that the lateral resolution was ≈40 to 60 nm in topographic images, and ≈100 to 200 nm in photocurrent images. These values were better than the classical limit of $\lambda/2 = 400$ nm, but still short of a real SNOM regime [6].

The samples studied in this first test experiment were obtained by electron gun evaporation of Pt on n-type GaP(001) sulfur doped substrates ($n = 5 \times 10^{17}$ cm^{-3}). The substrates were cleaned with hot organic solvents and in a 5% HCl solution during 1 minute and rinsed with deionized water. A 10 nm thick Pt film was deposited; the back Ohmic contacts consisted of a 62% Au–38% Sn alloy.

We now discuss some typical results, which are consistent with a much larger set of data not explicitly presented here. Fig. 3 shows typical microimages taken at the photon energy of 1.512 eV (laser diode source). In Fig. 3a, we see the topographic image over a 16×16 μm^2 area. The analyzed region presents lateral topographic variations on the scale of less than 1 μm. Dark-bright zones of the micrograph reveal profile variations of the sample surface of about 140 nm. Fig. 3b shows the scanning IPE micrograph of the same area. The brightest and darkest regions in our color scale correspond to photocurrents of 0.8 and ≈0.2 nA.

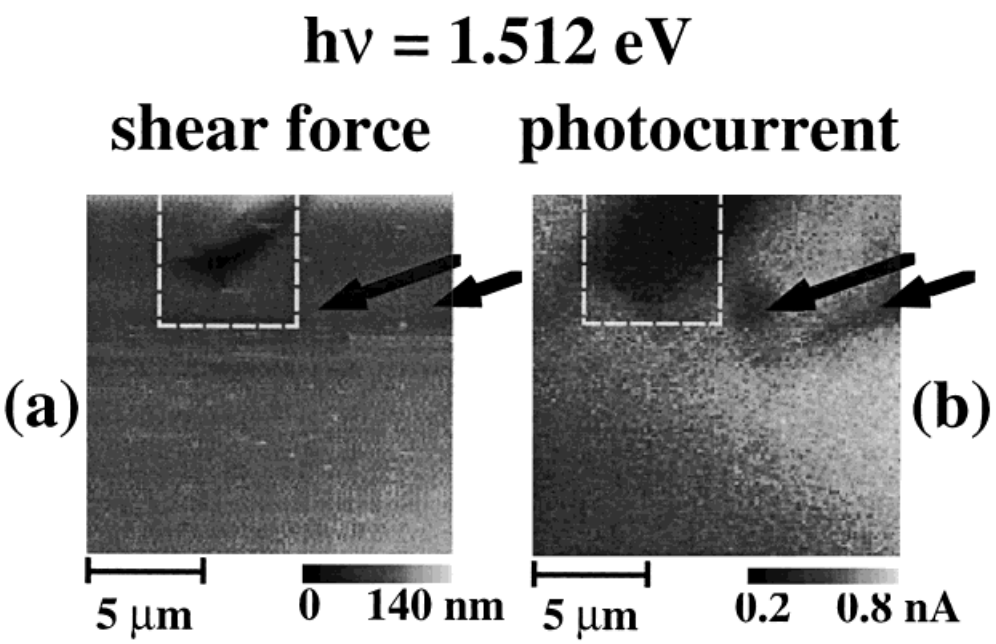

Fig. 3. Fig. 2 data from Ref. [7]: a) Shear-force topography and b) corresponding photocurrent microimage of a 16×16 μm^2 in constant distance mode. White pixels on the image are due to "jumps" of the tip. The width of the "dark" zone in the photocurrent image is $\approx$1.5 times larger than the corresponding defect

A comparison of Figs. 3a and b shows no one-to-one correspondence between their features: the feature in the marked square is present for both figures, whereas those emphasized by the arrows are only seen in Fig. 3b. We first consider the feature in the 6×6 μm^2 marked square: since it is seen in Fig. 3a, this feature must be of topographic origin (and not due, for example, to compositional variations). Its presence in Fig. 3b suggests that it is due to a scratch on the substrate. We can in fact hypothesize that the scratch results in local variations in the Pt overlayer thickness, which in turn create the contrast in the photocurrent micrograph, Fig. 3b.

We now consider the features marked by arrows in Fig. 3b, which are not present in Fig. 3a and therefore cannot have topographic origin. The main non-topographic cause of the IPE intensity inhomogeneities are the local fluctuations in the electron–hole recombination rate. A strong interface recombination was independently confirmed by I–V measurements: the ideality factor was larger than two and the saturation current was much higher than the expected value for a barrier of 1.41 eV (see below).

We proved that this approach is capable to locally explore the interface energy barriers – Schottky barrier heights in the present case. Typical results are reported in Fig. 4. Fig. 4a shows the topographic and photocurrent intensity images taken at $h\nu = 1.465$ eV. Fig. 4b shows the square root of the photocurrent versus photon energy (Fowler plot) [11] taken in points A and B of the photocurrent image. The photocurrent threshold position corresponds to the Schottky barrier height. From a linear fit, we obtain Schottky barrier heights of 1.409 and 1.413 eV. The comparison of the thresh-

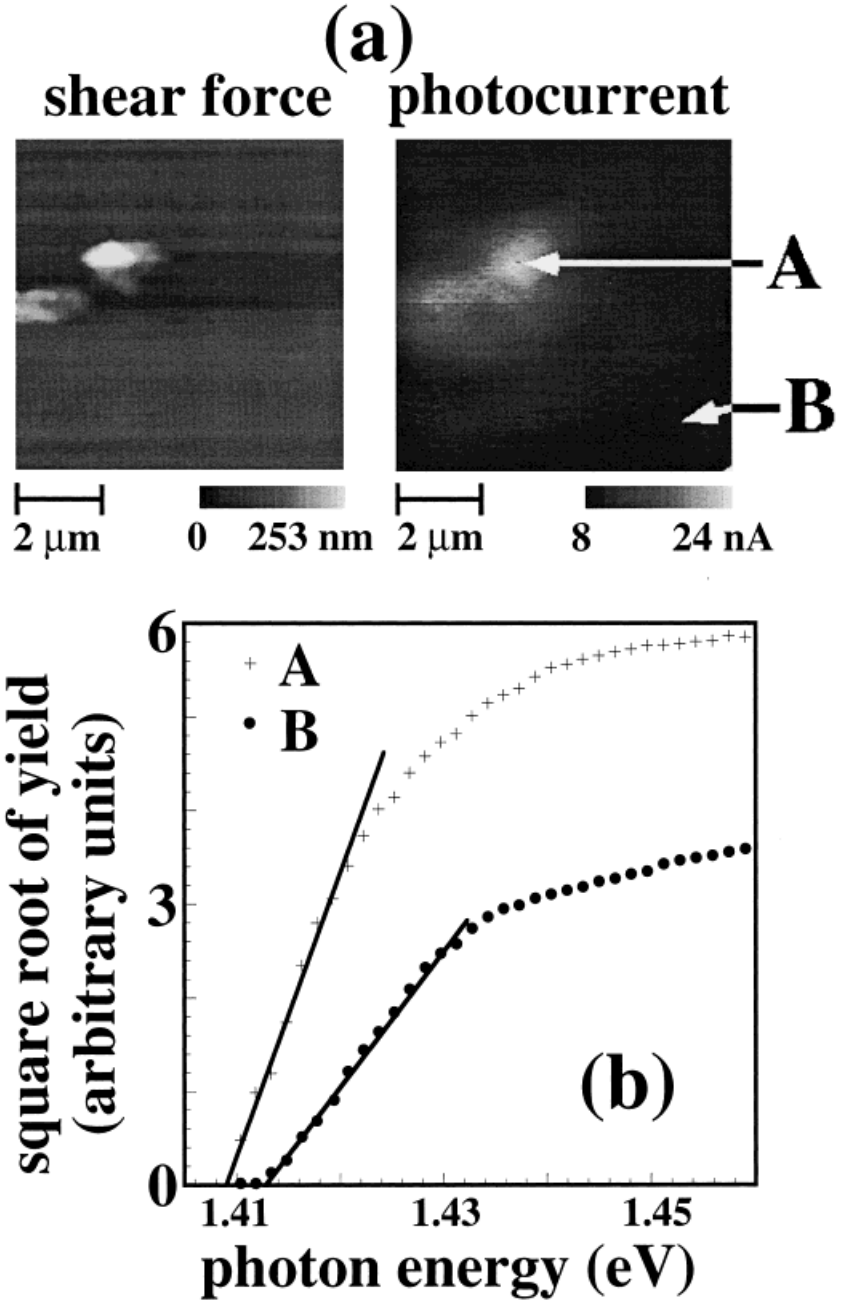

Fig. 4. Again from Ref. [7]: a) Shear-force topography and photocurrent microimages in a 8×8 μm^2 zone taken at $h\nu$ = 1.465 eV. b) The square root of the internal photoemission yield vs. photon energy for the Pt/n-GaP(001) Schottky barrier at 300 K measured in a "bright" (A) and "dark" (B) zone

olds in Fig. 4 clearly indicates that this difference is beyond the experimental uncertainty, which we estimate from the fit not to exceed ±1 meV.

We note, however, that these Schottky barrier lateral variations cannot be the main cause of the large photocurrent intensity fluctuations on the right-hand side of Fig. 4a. Assuming that thermionic emission is dominant in the $I-V$ characteristics, a variation of 4 meV of the Schottky barrier height induces a photocurrent intensity variation of ≈15%, whereas the observed variations are much larger, of the order of 250 to 300%.

As already mentioned, these large intensity variations can be explained instead by lateral changes of the recombination rate – probably related to microchemical inhomogeneities like those which were recently detected by photoemission spectromicroscopy [1]. Note that inhomogeneities are expected for chemically cleaned III–V substrates, as revealed for example by BEEM studies [12].

These first tests [7] were, in summary, successful in demonstrating that a combination of IPE and SNOM can study the lateral variations of different properties of a solid interface. Subsequent experiments extended this approach to other systems, e.g., to the $Au/SiN_x/GaAs(100)$ and PtSi/Si interfaces.

4. Scanning Near-Field Optical Microscopy (SNOM) Tests

One issue, however, remained unanswered: could one reach a SNOM regime while using an FEL rather than a conventional photon source? This question was removed by more recent and very successful tests [8].

The first SNOM experiments with an FEL were performed at the Vanderbilt FEL center [8] and measured the local reflectivity of a PtSi/Si system. The reflectivity in SNOM images revealed features that were not present in the corresponding shear-force (topology) images and which were due to localized changes in the bulk properties of the sample. The size of the smallest detected features clearly demonstrated that near-field conditions were reached. The use of different photon wavelengths (0.63, 1.2 and 2.4 μm) enabled us to probe regions of different depth. These tests were of course quite important because of the growing interest in SNOM techniques [6 to 8, 10].

As already mentioned, the local FEL-SNOM reflectivity measurements were complemented by shear-force measurements [6 to 8, 10] revealing the corresponding local surface topology. This enabled us to distinguish topological features from true lateral variations of the optical properties of the sample.

Fig. 5 shows the FEL-SNOM experimental set-up. The Vanderbilt FEL electron beam is produced by a 45 MeV radiofrequency accelerator, operating at a frequency up to 2.856 GHz. The emitted infrared radiation is continuously tunable over the 2 to 10 μm wavelength (extended to 1 μm by second-harmonic generation) with high output power and brightness. Pulses with 6 ms duration, 360 mJ energy, and 11 W average power (repetition rate 30 Hz) were reliably demonstrated for 4.8 mm wavelength.

Our SNOM [13] is a two-piece cylinder, similar to the atomic-force microscope (AFM) we described in Ref. [14]. The detection system is on the upper part and the sample scanning devices in the lower part. The piezoelectric scanning range is $17 \times 17 \times 5\ \mu m^3$. The tip–sample distance is controlled by a shear-force feedback system [10] and the topographic vertical resolution is 1 nm. The tip of the optical fiber was stretched obtaining a few tens of nanometer wide pinhole.

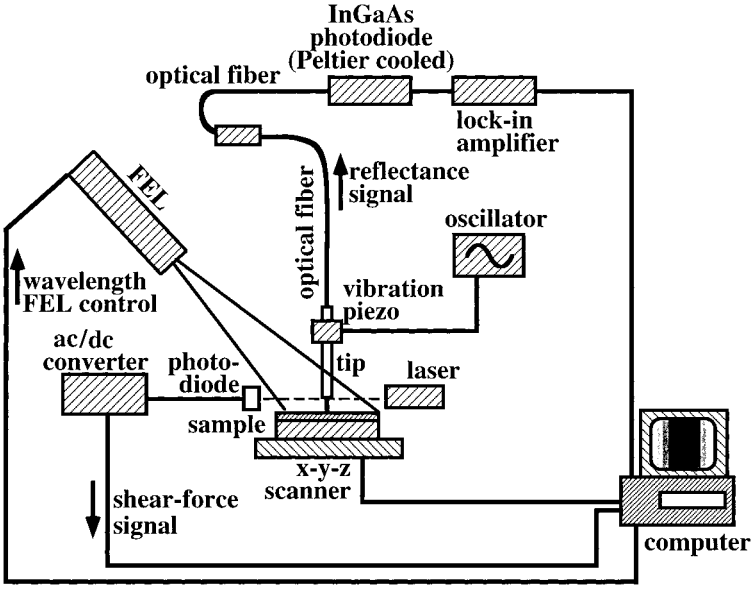

Fig. 5. Scheme of the experimental set-up of Ref. [8]

Infrared reflectivity images were obtained by detecting the reflected intensity while scanning the fiber position relative to the sample. We used two different FEL wavelengths: 1.2 and 2.4 μm. In addition, we also performed experiments with a 5 mW He–Ne laser (0.63 μm wavelength). The reflectivity was measured with a standard lock-in technique. Topographic images were obtained by measuring the shear-force signal with a synchronous detection including a piezoelectric oscillator and an ac/dc converter [15].

Successful tests were performed studying a PtSi/Si system, obtained by evaporating 4 nm of Pt on a Si substrate (previously cleaned with standard techniques) at room temperature. The sample was then annealed at 350 °C to form the interface.

Fig. 6a is a 12×12 μm^2 shear force image. Brighter areas correspond to higher topography values (or to higher reflectivity in the optical images shown later). No filtering was performed except for a background and plane alignment.

A rather big structure (corrugation 1500 nm) is visible in the upper left corner. This is an anomalous feature: the shear-force images are in general quite smooth with corrugation not exceeding a few tens of nanometers. However, the strongly corrugated area was also visible in the optical images, thus we used it to correlate the two types of images. Fig. 6b shows the portion of Fig. 6a below the strongly corrugated area with a different dynamic range, revealing weaker topographic contrast and in particular a round structure with 150 nm corrugation.

Fig. 7a is a reflectivity image of the same area of Fig. 6a for 2.4 μm wavelength. The strongly corrugated feature is still visible, but in addition we see a 1000 nm wide, 0.2 mV deep transversal "valley". Note that the "valley" is not at all correlated to topographic structure. Furthermore, due to the deep penetration of the infrared light its origin must be well below the surface; we tentatively attribute it to a Si groove. The corrugation on the surface does not appear to influence in this case the reflectivity contrast.

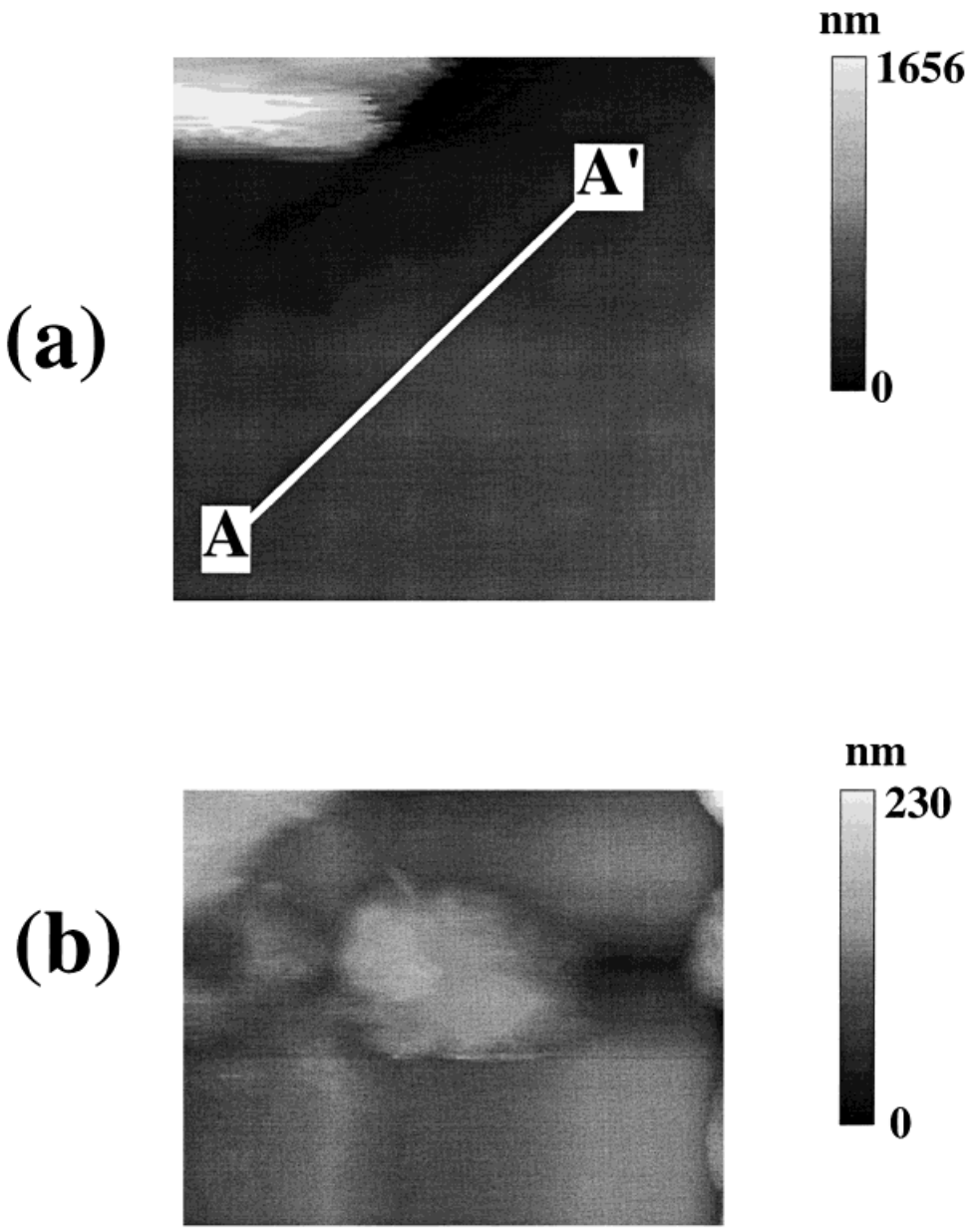

Fig. 6. Data from Ref. [8]: a) 12×12 μm^2 shear-force topography image; b) shear-force image taken from the lower part of the previous figure

Fig. 7b is a reflectivity image similar to Fig. 6a for 1.2 μm wavelength. The transverse "valley" of purely optical origin is still clearly visible. This is no longer true for the image of Fig. 7c, taken at 0.63 μm wavelength, whereas the strongly corrugated upper-left-corner structure is still visible.

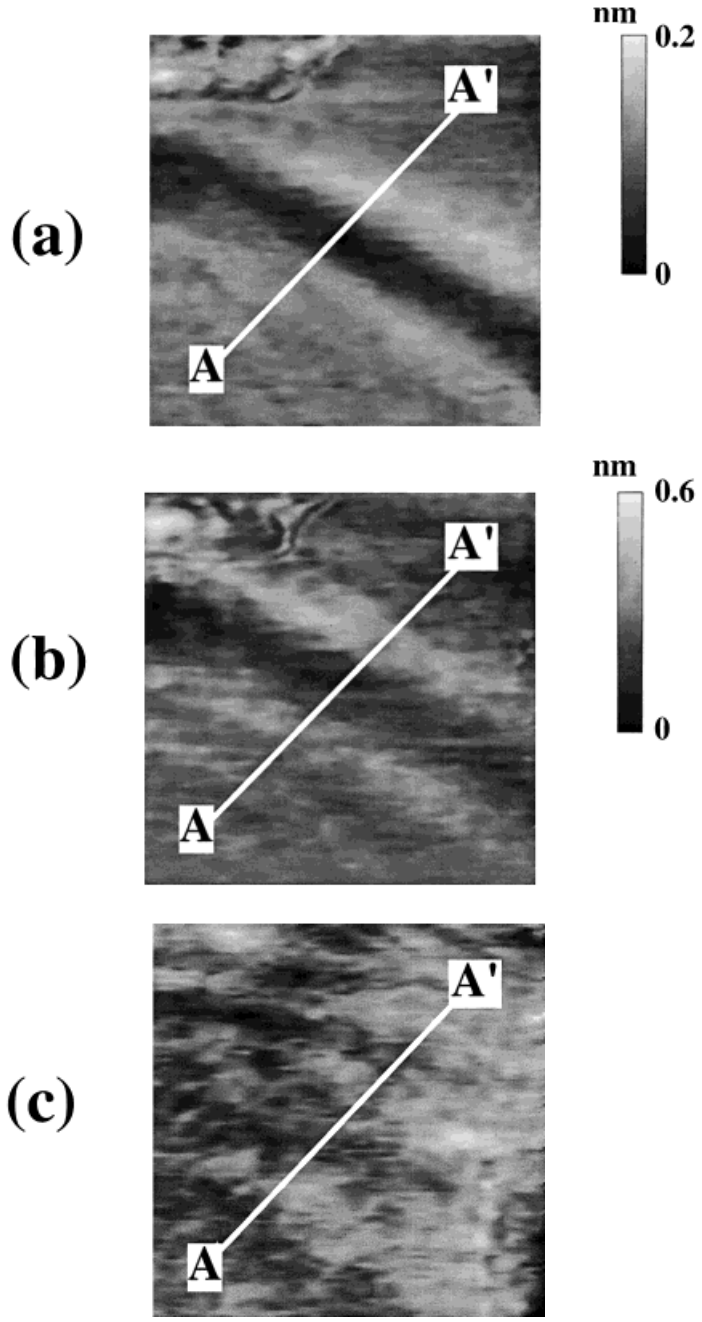

Fig. 7. a) Reflectivity image corresponding to Fig. 6a, taken with a photon wavelength of a) 2.4, b) 1.2, and c) 0.63 μm

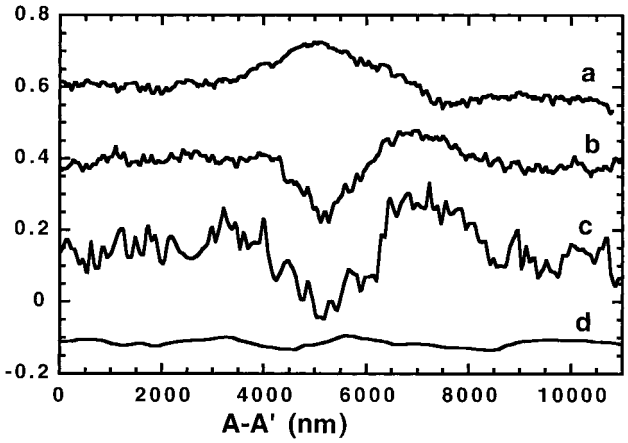

Fig. 8. Profiles along the marked lines in a) the topography Fig. 6a; b) to d) the optical-reflectivity Fig. 7

Fig. 8 shows the line contours taken along the marked lines of Figs. 6a and 7. The topographic line (curve a) reveals a corrugation of 150 nm. Lines b (Fig. 7a) and c (Fig. 7b) show the reflectivity minimum of the "valley". Line d (Fig. 7c) shows no reflectivity variations within the experimental uncertainty. This indicates that the "valley" in the 2.4 and 1.2 μm images is deeper than the maximum penetration of 0.63 μm photons at our incidence angle of 75° from the normal direction.

The "valley" observed in Figs. 7a and b could be due to the silicon–silicide interface. This possibility is being tested by an extention of the same approach to other infrared spectroscopy modes, thanks to the flexibility of our multi-purpose SNOM module [13]. We already obtained some photocurrent images by illuminating the sample through the optical fiber. A similar approach can be used to detect very small lateral variations of interface barrier heights [16].

An upper limit for the lateral resolution was estimated from the edge slope of the smallest detected features in a large number of images. We conclude that the resolution was better than 100 nm for topographic images, and than 200 to 400 nm for reflectivity images. Although these values, in the best case better than $\lambda/10$ (240 nm), are most likely underestimates, they are already well below the $\lambda/2$ level, demonstrating that the main objective of near-field conditions was achieved.

The first tests of this novel FEL-SNOM combination are quite encouraging. No major problems were encountered, a near-field condition was clearly achieved, and the technique appears feasible to a huge variety of buried interface studies. The combination of reflection and shear-force measurements provides a clear distinction between topographic variations at the surface and variations in the optical properties.

5. A Look at the Future

The previously described successful tests open the way to measurements of lateral variations of interface barriers for a huge variety of systems, These systematic studies are the most obvious development avenue for the research. Their results should provide a

clear picture of lateral variations in interface properties and of their influence on the behavior and performance of microelectronic devices.

Other parallel avenues, however, could be envisaged, such as time-resolved experiments and studies with even higher energy and/or lateral resolution, or parallel use of photoemission techniques to explore the link between lateral barrier fluctuations and local chemical properties [1 to 3].

Such developments will be undoubtedly helped by the implementation of better instrumentation and in particular of better photon sources. These should include conventional, broadly-tunable lasers as well as novel FELs. We also note the forthcoming tests of ultraviolet (and possibly X-ray) FELs based on the Self-Amplified Spontaneous Emission (SASE) mechanism [17].

These machines could increase the peak brightness by many orders of magnitude with respect to the present synchrotron sources. On the other hand, they could also be easily synchronized to infrared FELs, opening the way to a variety of novel and exciting experiments on interfaces.

In summary, interface research is definitely beyond the somewhat primitive stage of imagining the interface parameters as constants for the entire interface. This picture, forced upon the researchers by the lack of suitable probes, is in sharp conflict with the mounting experimental evidence for lateral barrier fluctuations. FEL-SNOM experiments appear as a very promising – and potentially the best – approach to attack this problem. Their results will probably make it impossible to think about semiconductor interfaces in the old and overidealized way.

Acknowledgements The authors thank D. W. Pohl, and G. Clerc, A. Bitz, E. Tuncel, J. L. Staehli and the entire staff of the Vanderbilt FEL for useful interactions and essential support. Work was supported by the Italian National Research Council, by the US Office of Naval Research, by the Fonds National de la Recherche Scientifique, by the Ecole Polytecnique Fédérale de Lausanne and by the Ministère de la Recherche et de l'Enseignement Supérieur (France).

References

[1] G. MARGARITONDO, Progr. Surf. Sci. **4**, 311 (1997), and references therein.
[2] M. ZACCHIGNA, L. SIRIGU, J. ALMEIDA, H. BERGER, L. GREGORATTI, M. MARSI, M. KISKINOVA, and G. MARGARITONDO, Appl. Phys. Lett. **73**, 1859 (1998).
[3] J. ALMEIDA, I. VOBORNIK, H. BERGER, M. KISKINOVA, A. KOLMAKOV, M. MARSI, and G. MARGARITONDO, Phys. Rev. B **55**, 4899 (1997).
[4] L. D. BELL, W. J. KAISER, M. H. HECHT and L. C. DAVIES, in: Scanning Tunneling Microscope, Eds. J. A. STROSCIO and W. J. KAISER, Academic Press, Boston 1993 (p. 307).
H. PALM, M. ARBES, and W. SCHULZ, Phys. Rev. Lett. **71**, 2224 (1993).
R. H. WILLIAMS, Appl. Surf. Sci. **70/71**, 386 (1993).
A. A. TALIN, R. S. WILLIAMS, B. A. MORGAN, K. M. RING, and K. L. KAVANAGH, Phys. Rev. B **49**, 16474 (1994).
A. BAUER, M. T. CUBERES, M. PRIETSCH, and G. KAINDL, J. Vac. Sci. Technol. B **11**, 4 (1993).
R. LUDEKE, M. PRIETSCH, and A. SAMSAVAR, J. Vac. Sci. Technol. B **9**, 2342 (1991).
[5] C. COLUZZA, E. TUNCEL, J.-L. STAEHLI, P. A. BAUDAT, G. MARGARITONDO, J. T. MCKINLEY, A. UEDA, A. V. BARNES, R. G. ALBRIDGE, N. H. TOLK, D. MARTIN, F. MORIER-GENOUD, C. DUPUY, A. RUDRA, and M. ILEGEMS, Phys. Rev. (Rapid Commun.) B **46**, 12834 (1992).
J. T. MCKINLEY, R. G. ALBRIDGE, A. V. BARNES, P. A. BAUDAT, G. C. CHEN, C. COLUZZA, J. L. DAVIDSON, C. DUPUY, F. GOZZO, M. ILEGEMS, M. L. LANGUELL, D. MARTIN, F. MORIER-GENOUD,

P. L. Polavarapu, A. Rudra, J. F. Smith, E. Tuncel, X. Yang, A. Ueda, G. Margaritondo, and N. H. Tolk, Nucl. Instrum. and Methods A **341**, 156 (1994).
J. T. McKinley, R. G. Albridge, A. V. Barnes, A. Ueda, N. H. Tolk, C. Coluzza, F. Gozzo, G. Margaritondo, D. Martin, F. Morier-Genoud, C. Dupuy, A. Rudra, and M. Ilegems, J. Vac. Sci. Technol. B **11**, 1614 (1993).
J. T. McKinley, R. G. Albridge, A. V. Barnes, G. C. Chen, J. L. Davidson, M. L. Languell, P. L. Polavarapu, J. F. Smith, X. Yang, A. Ueda, N. Tolk, C, Coluzza, P. A. Baudat, C. Dupuy, F. Gozzo, M. Ilegems, D. Martin, F. Morier-Genoud, A. Rudra, E, Tuncel, and G. Margaritondo, J. Vac. Sci. Technol. A **12**, 2323 (1994).
N. H. Tolk, J. T. McKinley, and G. Margaritondo, Surf. Rev. Lett. **2**, 501 (1995).
[6] D. W. Pohl and D. Courjon (Eds.), Near Field Optics, Kluwer, Dordrecht 1993.
E. Betzig and J. K. Trautmann, Science **2576**, 189 (1992).
S. K. Buratto, J. W. P. Hsu, E. Betzig, J. T. Trautman, R. B. Bylsma, C. C. Bahr, and M. J. Cardillo, Appl. Phys. Lett. **65**, 21 (1994).
[7] J. Almeida, Tiziana Dell'Orto, C. Coluzza, G. Margaritondo, O. Bergoss, M. Spajer, and D. Courjon, Appl. Phys. Lett. **69**, 2361 (1996).
[8] A. Cricenti, R. Generosi, P. Perfetti, J. M. Gilligan, N. H. Tolk, C. Coluzza, and G. Margaritondo, Appl. Phys. Lett. **73**, 151 (1998).
[9] E. Betzig, P. L. Finn, and J. S. Wiener, Appl. Phys. Lett. **60**, 2484 (1994).
[10] O. Bergossi and M. Spajer, Conf. Interferometry 94, Warsaw 1994, Proc. SPIE **2341**, 239 (1994).
[11] R. H. Fowler, Phys. Rev. **38**, 45 (1931).
[12] L. D. Bell, W. J. Kaiser, M. H. Hecht, and L. C. Davies, in: Scanning Tunneling Microscope, Eds. J. A. Stroscio and W. J. Kaiser, Academic Press, Boston 1993 (p. 307).
[13] A. Cricenti, R. Generosi, C. Barchesi, M. Luce, and M. Rinaldi, Rev. Sci. Instrum. **69**, 3240 (1998).
[14] A. Cricenti and R. Generosi, Rev. Sci. Instrum. **66**, 2843 (1995).
[15] C. Barchesi, A. Cricenti, R. Generosi, C. Giammichele, M. Luce, and M. Rinaldi, Rev. Sci. Instrum. **68**, 3799 (1997).
[16] C. Coluzza, J. Almeida, T. Dell'Orto, O. Bergossi, M. Spajer, S. Davy, D. Courjon, A. Cricenti, R. Generosi, P. Perfetti, and G. Faini, Proc. SPIE **2782**, 591 (1997).
[17] R. Bonifacio, C. Pellegrini, and L. Narducci, Opt. Commun. **50**, 373 (1984); A VUV Free Electron Laser at the TESLA Test Facility at DESY – Conceptual Design Report, TESLA-FEL 95-03, DESY Print, Hamburg 1995.